Hindawi Publishing Corporation
Discrete Dynamics in Nature and Society
Volume 2016, Article ID 4961681, 10 pages
http://dx.doi.org/10.1155/2016/4961681

Research Article

Research on the Effects of Heterogeneity on Pedestrian Dynamics in Walkway of Subway Station

Haoling Wu,[1] Zhenzhou Yuan,[1] Huixuan Li,[1] and Junfang Tian[2]

[1] *MOE Key Laboratory for Urban Transportation Complex Systems Theory and Technology, Beijing Jiaotong University, Beijing 100044, China*
[2] *Institute of Systems Engineering, College of Management and Economics, Tianjin University, Tianjin 300072, China*

Correspondence should be addressed to Haoling Wu; haoling_0715@126.com

Received 21 March 2016; Revised 18 May 2016; Accepted 29 May 2016

Academic Editor: Douglas R. Anderson

The major objective of this paper is to study the effects of heterogeneity on pedestrian dynamics in walkway of subway station. We analyze the observed data of the selected facility and find that walking speed and occupied space were varied in the population. In reality, pedestrians are heterogeneous individuals with different attributes. However, the research on how the heterogeneity affects the pedestrian dynamics in facilities of subway stations is insufficient. The improved floor field model is therefore presented to explore the effects of heterogeneity. Pedestrians are classified into pedestrians walking in pairs, fast pedestrians, and ordinary pedestrians. For convenience, they are denoted as *P*-pedestrians, *F*-pedestrians, and *O*-pedestrians, respectively. The proposed model is validated under homogeneous and heterogeneous conditions. Three pedestrian compositions are simulated to analyze the effects of heterogeneity on pedestrian dynamics. The results show that *P*-pedestrians have negative effect and *F*-pedestrians have positive effect. All of the results in this paper indicate that the capacity of walkway is not a constant value. It changes with different component proportions of heterogeneous pedestrians. The heterogeneity of pedestrian has an important influence on the pedestrian dynamics in the walkway of the subway station.

1. Introduction

Pedestrian dynamics plays an important role in the study of pedestrian flow, crowd evacuations, and so on. The research of the pedestrian dynamics in walkways focuses on the self-organization phenomenon [1–3] and jamming transition [4–9]. A variety of simulation models have been developed to study the pedestrian dynamics, such as social force model [1, 10–12], cellular automaton (CA) model [13–17], lattice gas model [18–20], and multiagent model [21, 22]. CA model has been widely used because of its simple rules and good performance for reproducing various self-organization phenomena. In [3, 23–25], a more sophisticated CA model—floor field model—has been introduced, which by now has become the standard CA approach to pedestrian dynamics [26]. In this model, there are two kinds of floor field, that is, static and dynamic ones. The static floor field is constant in time and represents the constant properties of the infrastructure. The dynamic floor field describes the dynamic interactions between the pedestrians. Furthermore, it has its own dynamics, namely, diffusion and decay, which leads to dilution and finally the vanishing of the trace after some time [23].

To determine the adequacy of the proposed model, it is essential to execute the process of validation. Validation has two types, qualitative and quantitative. Tsiftsis et al. [27] proposed a cellular-automata-based model that estimates the movement of individuals. The efficiency of the model has been thoroughly validated with qualitative major characteristics of crowd behavior and quantitative flow-density dependence. Georgoudas et al. [28] made use of empirical and simulation results to clarify the operation of the anticipative crowd management system and evaluate its efficiency. Klüpfel and Meyer-König [29] validated the presented model through comparing the flow-density fundamental diagram of the simulation result with the empirical one and calibrated six parameters. Wąs et al. [30] proposed a new discrete model and validated the model with fundamental diagram.

Qu et al. [31] validated the presented microscopic spatial-continuous model with walking speed, flow characteristics, lane forming behavior, and fundamental diagram. Campanella et al. [32] proposed a simple validation procedure that combines qualitative and quantitative assessments.

Most of these existing models treated pedestrian crowd as a collection of the same isolated individuals, that is, homogeneous pedestrians, which does not coincide with the reality. In reality, the pedestrian flow is composed of heterogeneous people with different individual attributes, including gender, age, luggage, and walking together or not. Their attributes reflect different microscopic traffic characteristics involving occupied space, speed, stride, stride frequency, and so forth. At present, some scholars have put their efforts to research the effects of heterogeneity on pedestrian flow. Lu et al. [33] proposed an extended floor field CA model to incorporate into the walking behavior of pedestrian groups and found the walking behavior of groups has an important but negative influence on pedestrian flow dynamics, especially when the density is at a high level. Campanella et al. [34] chose desired speed, body size, and reaction time as the heterogeneity parameters. Their simulation results strongly indicate that the impact of heterogeneity is very important and should not be neglected in modeling and analyzing pedestrian flow operations. Matsumoto et al. [35] analyzed the heterogeneous pedestrians of a high demand pedestrian crossing in downtown Tokyo. They have found that pedestrians, depending on their desired speeds, are scanning a certain area to choose their directions and that the changes of direction are getting smaller with increasing speed.

Till now, the effects of heterogeneity in walking facilities of subway stations have not been analyzed. And the floor field CA model has not included the pedestrian heterogeneity completely. Therefore, the major objective of this paper is to research the effects of heterogeneity on pedestrian dynamics by improving the floor field model. The rest of this paper is organized as follows. Section 2 presents the results of the field data and analyzes the characteristics of heterogeneous pedestrian flow. The details of the improved floor field model are introduced in Section 3. The simulation scenario is given in Section 4. Section 5 provides the simulation results to analyze the effects of heterogeneity on pedestrian dynamics. At last, the conclusions are summarized and the direction for future work is illustrated.

2. Data Collection and Characteristics of Heterogeneous Pedestrian Flow

A walkway of Beijing Xizhimen subway station was selected as the observation site. The width and the length of this facility are 3.6 m and 10.4 m (Figure 1), respectively. Two HD cameras were used to record the pedestrian flow for an hour during the peak time of a workday simultaneously. In our observations, 404 pedestrians (213 males, 191 females) were collected in the walkway. Most of the pedestrians were young and middle-aged people, and their ages mostly ranged from 15 to 60 years. The proportion of children and the elderly was very low. In our observations, 19% of the pedestrians walk

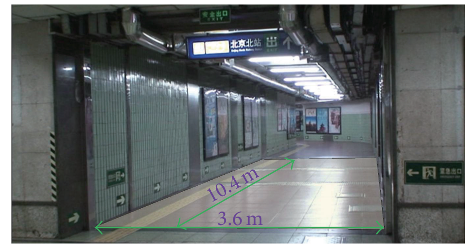

Figure 1: The snapshot of the selected walkway.

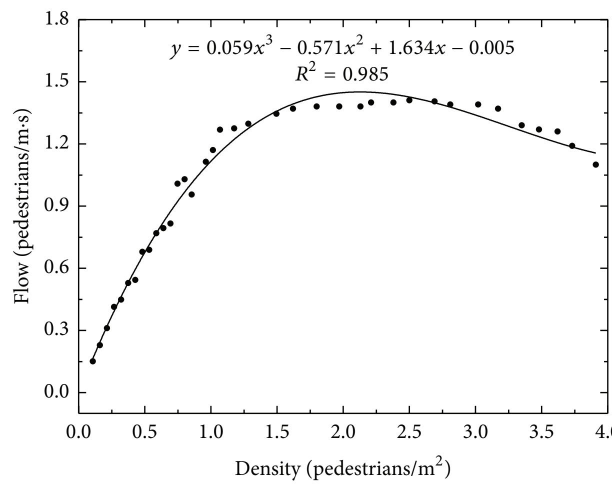

Figure 2: Flow-density fundamental diagram of the observed data.

in pairs, 6% of the pedestrians carry large luggage, and more than one-third of the people walk fast.

The scatter plot of flow-density based on the observed data in the walkway was drawn in Figure 2. The cubic equation is used to fit the curve and the result is good because the goodness of fit is 0.985. The capacity of this facility can be calculated through the flow-density model [36, 37]. The flow continually grows with the density when it is less than 2.2 pedestrians/m^2. When the density reaches 2.2 pedestrians/m^2, the flow of the walkway gets the maximum value and the capacity is 1.45 pedestrians/m·s. Then, the flow begins to decrease with the increasing density. The increasing gradient of pedestrian flow is greater than the decreasing one.

We extracted the heterogeneous attributes of pedestrians from the video and organized them in the form of individual cases afterward. Each pedestrian was recorded by individual characteristics, including gender, age, luggage, walking time, and walking in pairs or not. According to the statistical analysis of the observed data, different individual attributes of pedestrians reflect different microscopic traffic characteristics, involving speed, stride, stride frequency, occupied space, and so forth. We select walking speed and occupied space as indicators to represent the pedestrian heterogeneity. All of the observed pedestrians are classified into four classes according to the heterogeneous indexes. The categorization of pedestrians is shown in Table 1. The data listed in Table 1 come from the statistical analysis of the observation video.

Table 1: Categorization of pedestrians.

Categorization	Characteristics	Average walking speed (m/s)	Average occupied space (m^2/pedestrian)	Proportion (%)
Pedestrians walking in pairs	Two pedestrians walking together, hand in hand (arm in arm), talking with each other, holding a baby, and so forth.	1.15	0.32	19
Pedestrians with large luggage	Pedestrians who carry large luggage, including a suitcase, hiking bag, and stroller. The occupied space by the luggage is approximately equal to the occupied space by one pedestrian.	1.15	0.30	6
Fast pedestrians	Pedestrians walk alone and fast, and they do not carry or only carry small baggage.	1.57	0.16	35
Ordinary pedestrians	Pedestrians walk alone at a normal speed and do not carry or only carry small baggage.	1.16	0.16	40

Pedestrians who walk in pairs and those with large luggage have the same walking speed and they occupy almost the same spaces. These two classes of pedestrians can be regarded as one class and be collectively called pedestrians walking in pairs. For convenience, pedestrians walking in pairs, fast pedestrians, and ordinary pedestrians are denoted as P-pedestrians, F-pedestrians, and O-pedestrians in the rest of this paper.

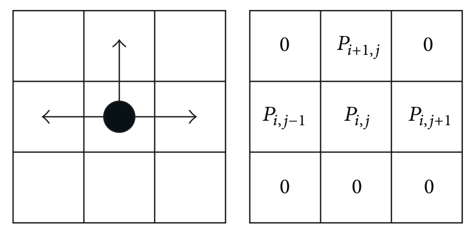

Figure 3: Moving directions and transition probabilities of pedestrians.

3. Model Development

3.1. Floor Field Model (FF Model) Introduction. The floor field model (FF model) [23–25] is defined on a two-dimensional square lattice where each cell can be occupied by at most one particle (pedestrian). In every time step, each particle is allowed to stay at its current position or move to one of the neighboring cells according to certain transition probabilities (1) given that the destination cell is not occupied by another particle. This is done synchronously for all particles (parallel update). The number of nearest neighbors on the lattice can be either four (von Neumann neighborhood) or eight (Moore neighborhood) [3]:

$$p_{ij} = N \exp\left(k_D D_{ij}\right) \exp\left(k_S S_{ij}\right) \left(1 - n_{ij}\right) \xi_{ij} \quad (1)$$

with occupation number $n_{ij} = 0, 1$; if the cell is occupied by other particles, the value is 1; otherwise, it is 0. Obstacle number is $\xi_{ij} = 0, 1$; if the cell is occupied by any obstacle, the value is 0; otherwise, it is 1.

N is a normalization factor for ensuring $\sum_{i,j} p_{ij} = 1$: $N = [\sum_{(i,j)} \exp(k_D D_{ij}) \exp(k_S S_{ij})(1 - n_{ij})\xi_{ij}]^{-1}$.

The probabilities p_{ij} are given by the interaction with two floor fields, static floor field S and dynamic floor field D. For the evacuation process, the static floor field S describes the shortest distance to the exit. The static floor field S does not evolve with time and is not changed by the presence of the pedestrians. Such a field can be used to specify regions of spaces which are more attractive, for example, an emergency exit or shop windows [24]. The dynamic floor field D was inspired by the motion of ants, which leave a pheromone trace. Other ants are able to smell this trail and follow it. This concept is adopted in this model. Each particle which moves from one cell to another leaves a virtual trace; that is, the value D_{ij} of the origin cell (i, j) increases by 1. Therefore, D has only nonnegative integer values. This trace acts attractively for other particles due to larger transition probabilities according to (1). The effect is that particles have a tendency to follow each other [38]. The D has its own dynamics, namely, diffusion and decay controlled by two parameters $\alpha \in [0, 1]$ and $\delta \in [0, 1]$, which means broadening and dilution of the trace. k_S and k_D are two positive parameters for scaling S_{ij} and D_{ij}, respectively. $k_S \in [0, \infty)$ is the coupling to the static floor field which characterizes the knowledge of the shortest path to the exits or the tendency to minimize the costs due to deviation from a planned route. This considerably controls one's velocity and evacuation times. $k_D \in [0, \infty)$ is the coupling to the dynamic floor field which characterizes the tendency to follow other pedestrians (herding behavior) [39].

3.2. Heterogeneous Floor Field Model (HFF Model). The space is discretized into cells. In each time step, pedestrians move only one cell in the forward, left, or right directions or remain unmoved, and the backward direction is forbidden for pedestrians [33, 40, 41] in our HFF model (Figure 3). These two fields S and D determine the transition probabilities in such a way that a particle movement is more likely in the direction of higher fields.

3.2.1. Static Floor Field S. In case of the walkway considered here, the static floor field describes the shortest distance to the exit of the walkway. The values of S studied here are then calculated with a Manhattan distance metric. The explicit calculating process is as follows:

(1) The walkway is divided into a rectangular grid. All of the cells on the right side of the walkway shown in Figure 4 are the exit cells (except for the wall cells).

(2) Any cell which has the largest distance to the nearest exit cells is assigned a value 0, that is, the cells which are located on the left-most layer of the walkway (except for the wall cells) in Figure 4.

(3) Then, all adjacent cells to the previous one (a "second layer" of cells) are assigned the same value, according to the following rules: if a cell has value N, then adjacent cells are assigned the value $N + 1$.

(4) Then, the third layer of cells is calculated in the same way as the second layer.

(5) The process is repeated until all cells are evaluated.

(6) The value of wall cells is $S_w = -1$. It is beneficial to distinguish wall cells from other cells.

Figure 4 shows the static floor field obtained by applying this set of rules to the walkway of size $W \times L$ with exit cells on the right side, where W and L correspond to the width and the length of the walkway.

3.2.2. Dynamic Floor Field D. The dynamic floor field D has its own dynamics, namely, decaying with probability δ and diffusing with probability α. After each time step, it is updated according to

$$D_{ij}(t+1) = (1-\delta)\left[D_{ij}(t) + \frac{\alpha}{4}\Delta D_{ij}(t)\right], \qquad (2)$$

where

$$\begin{aligned}\Delta D_{ij}(t) = {} & D_{i,j+1}(t) + D_{i,j-1}(t) + D_{i+1,j}(t) + D_{i-1,j}(t) \\ & - 4D_{i,j}(t)\end{aligned} \qquad (3)$$

is a discretization of the Laplace operator. Equation (2) can also be obtained by discretizing

$$\frac{\partial}{\partial t}D_{xy}(t) = \beta\nabla^2 D_{xy}(t) - \delta D_{xy}(t), \qquad (4)$$

which is the diffusion equation with diffusion constant $\beta = \alpha(1-\delta)/4$ and an extra term for the decay. Here, $\nabla^2 = \partial^2/\partial x^2 + \partial^2/\partial y^2$ is the usual Laplace operator in two dimensions [3].

3.2.3. Update Rules. The update rules of HFF model have the following structure.

(1) P-pedestrians, F-pedestrians, and O-pedestrians are generated in the system with random positions. P-pedestrians are distributed in pairs and each group of them move together during the simulation process.

(2) The static floor field S of each cell is calculated according to the rules shown in Section 3.2.1.

(3) The dynamic floor field D of each cell decays with probability δ and diffuses with probability α to one of its neighboring cells.

(4) For each one of the F-pedestrians and O-pedestrians, the transition probabilities p_{ij} for a move to an unoccupied neighbor cell (i, j) are determined by the local dynamics and the two floor fields. The values of the fields S and D are weighted with two sensitivity parameters $k_S \in [0,\infty)$ and $k_D \in [0,\infty)$. This yields

$$p_{ij} = N\exp\left(k_D D_{ij}\right)\exp\left(k_S S_{ij}\right)p_I(i,j)\left(1-n_{ij}\right)\xi_{ij}. \qquad (5)$$

Normalization is as follows:

$$N = \left[\sum_{(i,j)}\exp\left(k_D D_{ij}\right)\exp\left(k_S S_{ij}\right)p_I(i,j)\left(1-n_{ij}\right)\xi_{ij}\right]^{-1}. \qquad (6)$$

Here p_I represents the inertia effect [23] for the direction of one's motion in the previous time step. In the walkway scenario considered in this paper, if a particle moved in the forward direction in the last time step, then p_I given by $p_I(i, j) = \exp(k_I)$, and $p_I(i, j) = 1$ for other directions, where k_I is the sensitivity parameter.

For P-pedestrians, when they want to move left or right, the calculating method of transition probabilities is the same with the isolated pedestrians. But for the case of moving forward, we should compare the transition probabilities $P^L_{i+1,j}$ and $P^R_{i+1,j}$ of the cells in front of each pair of P-pedestrians; then the greater one (Figure 5) is chosen as the transition probability to move forward.

(5) Each pedestrian chooses a target cell based on the transition probabilities p_{ij} determined in the previous step.

(6) The conflicts arising from any two or more pedestrians attempting to move to the same target cell are resolved by a probabilistic method [23]. The pedestrians which are allowed to move execute their step with their own speed, and the losers remain unmoved.

(7) D at the origin cell (i, j) of each moving particle is increased by one: $D^{t+1}_{ij} = D^t_{ij} + 1$.

4. Simulation Scenario

The size of the simulation scenario is the same with the real walkway, and the width and the length are 3.6 m × 10.4 m. We discretized the scenario into 9 × 26 cells each with a size of $0.4 \times 0.4\,\mathrm{m}^2$. The layout of the walkway is shown in Figure 6. There are three types of pedestrians in the system: P-pedestrians, F-pedestrians, and O-pedestrians. For simplicity, the speed of P-pedestrians and O-pedestrians is approximate to 1.2 m/s, and F-pedestrians' speed is approximate to 1.6 m/s. Each time step corresponds to 1/12 s. Pedestrians' position transition frequency in each time step reflects their speed. The fast pedestrians' position is updated once in three time steps, and the slow pedestrians' position is updated once in

−1	−1	−1	−1	−1	−1	−1	−1	−1	−1	−1	−1	−1	−1	−1	−1	−1	−1	−1	−1	−1	−1	−1	−1	−1	−1
0	1	2	3	4	5	6	7	8	9	10	11	12	13	14	15	16	17	18	19	20	21	22	23	24	25
0	1	2	3	4	5	6	7	8	9	10	11	12	13	14	15	16	17	18	19	20	21	22	23	24	25
0	1	2	3	4	5	6	7	8	9	10	11	12	13	14	15	16	17	18	19	20	21	22	23	24	25
0	1	2	3	4	5	6	7	8	9	10	11	12	13	14	15	16	17	18	19	20	21	22	23	24	25
0	1	2	3	4	5	6	7	8	9	10	11	12	13	14	15	16	17	18	19	20	21	22	23	24	25
0	1	2	3	4	5	6	7	8	9	10	11	12	13	14	15	16	17	18	19	20	21	22	23	24	25
0	1	2	3	4	5	6	7	8	9	10	11	12	13	14	15	16	17	18	19	20	21	22	23	24	25
0	1	2	3	4	5	6	7	8	9	10	11	12	13	14	15	16	17	18	19	20	21	22	23	24	25
0	1	2	3	4	5	6	7	8	9	10	11	12	13	14	15	16	17	18	19	20	21	22	23	24	25
−1	−1	−1	−1	−1	−1	−1	−1	−1	−1	−1	−1	−1	−1	−1	−1	−1	−1	−1	−1	−1	−1	−1	−1	−1	−1

Figure 4: Static floor field S for the walkway of size $W \times L$ with exit cells on the right side.

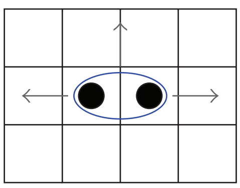

0	$P^L_{i+1,j}$	$P^R_{i+1,j}$	0
$P_{i,j-1}$	$P^L_{i,j}$	$P^R_{i,j}$	$P_{i,j+1}$
0	0	0	0

Figure 5: Moving directions and transition probabilities of P-pedestrians.

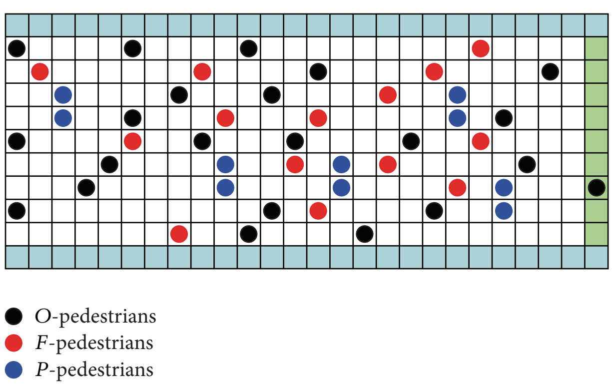

Figure 6: The random distribution of pedestrians at the initial time step.

four time steps. Every pair of P-pedestrians occupies two cells while each one of F-pedestrians and O-pedestrians occupies one cell. The periodic boundary is adopted to obtain the flows with different densities. Pedestrians are distributed randomly in the system at the initial time step (Figure 6).

5. Simulation Results

5.1. Model Validation. In order to verify the precision of the proposed model, we validated the model under homogeneous and heterogeneous situations. The capacity and the density-flow fundamental diagrams were reproduced to validate the model quantitatively. The corresponding polynomial trend lines of the observed data and the simulation results have been fitted and compared as shown in [27]. The percentage of the crowd varies from 0.1 to 0.99. The comparison between the observed data and the simulation results is shown in Figures 7(a) and 7(b).

Under the homogeneous situation, pedestrians are regarded as the same individuals with the average speed of 1.3 m/s when validating the model. Each time step corresponds to 4/13 s. In the process of the simulation, the parameters were set as $k_S = 2.0$, $k_D = 1$, $\alpha = 0.1$, $\delta = 0.4$, and $k_I = 3$. The simulation result shows that the capacity of the walkway is 1.48 pedestrians/m·s when the density is 2.48 pedestrians/m^2. The capacity error between the observed data (1.45 pedestrians/m·s) and the homogeneous simulation result is 2.07%.

There are P-pedestrians, F-pedestrians, and O-pedestrians in the system under the heterogeneous situation. The component percentage is 25%, 35%, and 40%. In the process of the simulation, the parameters were set as $k_S = 1.8$, $k_D = 1$, $\alpha = 0.1$, $\delta = 0.4$, and $k_I = 3$. The capacity of the simulation is 1.43 pedestrians/m·s when the density is 2.43 pedestrians/m^2. The capacity error between the observed data (1.45 pedestrians/m·s) and the heterogeneous simulation result is 1.38%.

Moreover, the corresponding polynomial trend lines of observed data and the simulation results of homogeneous and heterogeneous situations have been fitted in Figures 7(a) and 7(b), respectively. High values of goodness of fit (R^2) prove that trend lines fit the data sets quite well. The corresponding trend lines share common fundamental properties, regarding degree and end behavior. The capacity values and the fitting curves of the fundamental diagrams coincide well with the observed data, which support the idea that the proposed model is effective and feasible.

5.2. The Effects of P-Pedestrians on Pedestrian Dynamics. We analyze the effects of P-pedestrians on the pedestrian dynamics through research on the characteristics of the pedestrian flow which is formed with P-pedestrians and O-pedestrians. They have the same speed of 1.2 m/s. Each pair of the P-pedestrians occupy two cells and they move together during the simulation process. The percentage of the pedestrian flow increases from 0.1 to 0.99 gradually. The quantitative relationship of flow-density fundamental diagrams and the curve of capacity with different proportions of P-pedestrians can be obtained (Figures 8 and 9(a)).

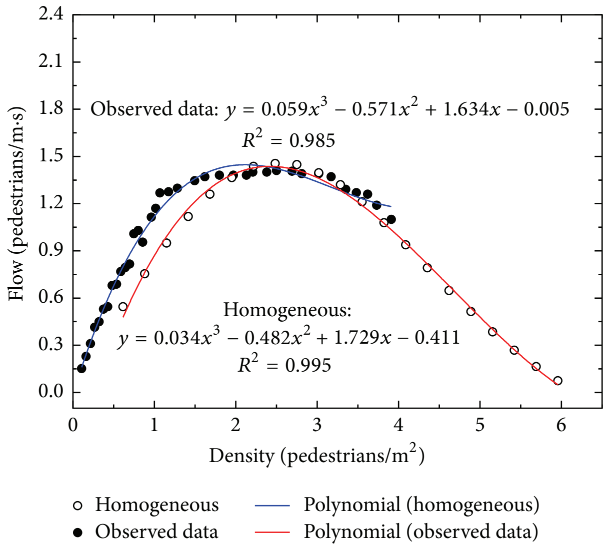

(a) Homogeneous situation

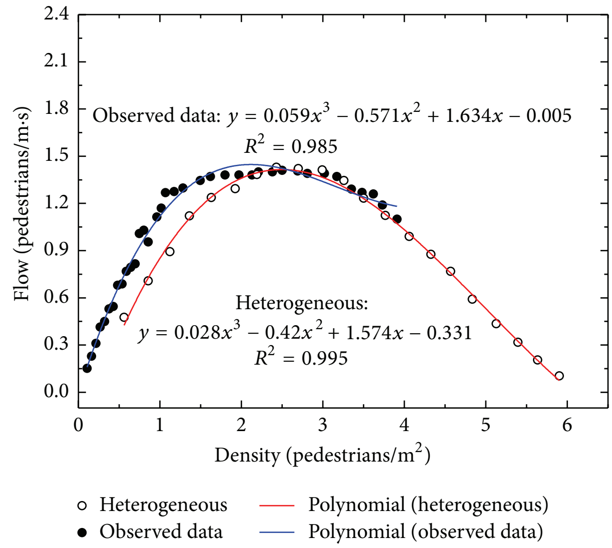

(b) Heterogeneous situation

FIGURE 7: Validation with the fundamental diagrams and capacity.

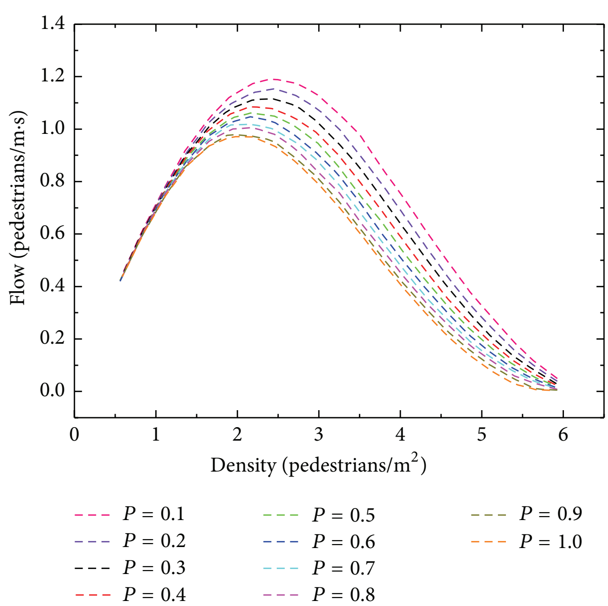

FIGURE 8: Fundamental diagrams of different proportions of P-pedestrians.

It is found out that P-pedestrians have great impact on the fundamental diagrams. In Figure 8, the differences among these curves are negligible when the density is less than 1.2 pedestrians/m^2. Then, when the density is more than 1.2 pedestrians/m^2, the gaps among them become large. The location of the fundamental diagrams descends and the capacity of the walkway declines gradually with the increasing percentage of P-pedestrians. The critical density corresponding to the capacity is moving left along the x-axis with the proportion of P-pedestrians increasing at the same time. It indicates that the phase transition occurs at the lower density with more P-pedestrians in the system.

We extract the capacity values from the fundamental diagrams and plot the curve shown in Figure 9(a). The capacity of the walkway is in the interval of $[0.97, 1.23]$. It always declines proportionally with the increasing percentage of P-pedestrians because the slope of the curve is nearly linear. The results indicate that P-pedestrians have negative effect on walkway capacity. The presence of this kind of pedestrians occupies more spaces and disturbs O-pedestrians during the walking process. It may retard the emergence of lane formation and makes the pedestrian flow unsteadily.

5.3. The Effects of F-Pedestrians on Pedestrian Dynamics. The pedestrian flow is composed of F-pedestrians and O-pedestrians in this simulation experiment. Their speeds are 1.6 m/s and 1.2 m/s, respectively. Each of them occupies one cell. The percentage of the pedestrian flow increases from 0.1 to 0.99 gradually. The quantitative relationship of flow-density fundamental diagrams and the curve of capacity values with different proportions of F-pedestrians can be obtained (see Figures 10 and 9(b)).

With the increasing percentage of F-pedestrians, the changed trend of the curves can be divided into three stages in Figure 10. In the first stage, the curves rise one by one when the proportion of F-pedestrians is less than 0.6. Then, three curves which are corresponding to the proportion values of 0.6, 0.7, and 0.8 almost overlap together. In the third stage, the two curves of 0.9 and 1.0 start to decline when the density is more than 2.2 pedestrians/m^2 and the 1.0 curve declines faster.

The plot of the capacity whose range is $[1.23, 1.72]$ is drawn in Figure 9(b). The capacity grows fast when the proportion is between 0 and 0.3. Then, the increasing speed of the curve becomes slow to almost close to 0 when the proportion is changing from 0.3 to 0.8. The curve begins to go down from the point corresponding to the proportion

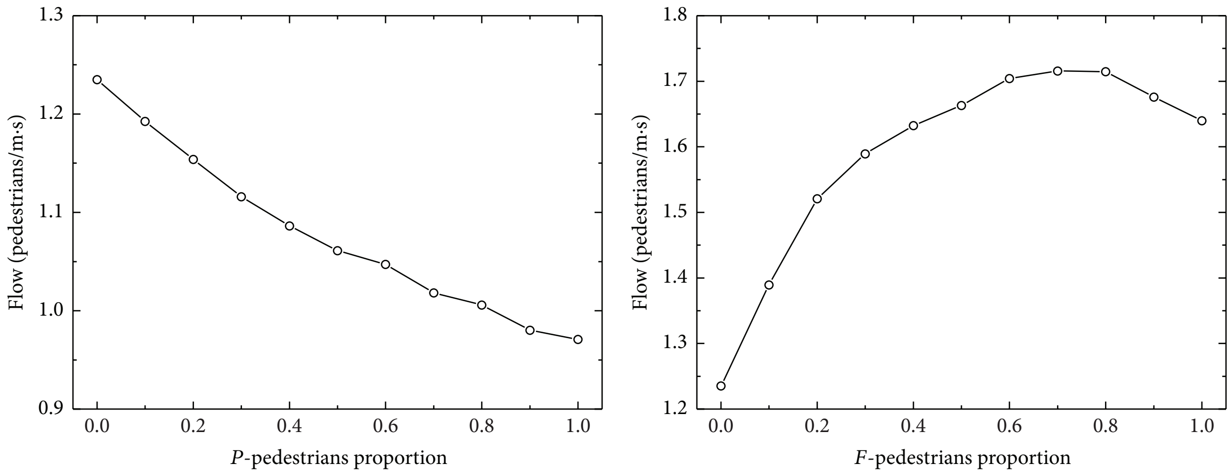

(a) Different proportions of P-pedestrians

(b) Different proportions of F-pedestrians

FIGURE 9: Capacity curves.

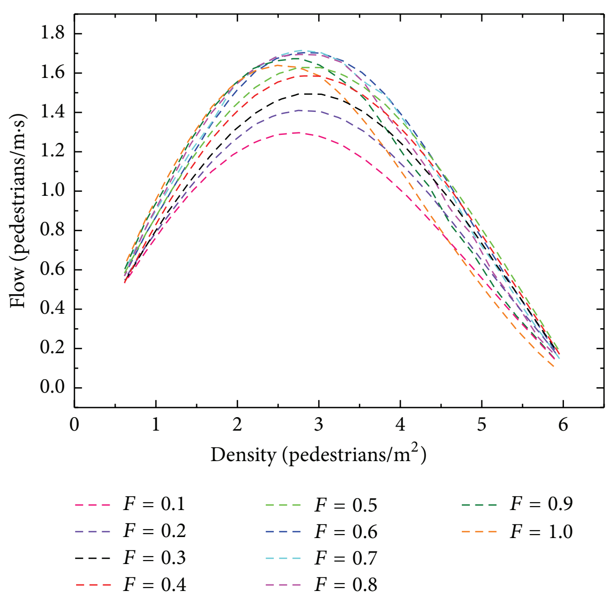

FIGURE 10: Fundamental diagrams of different proportions of F-pedestrians.

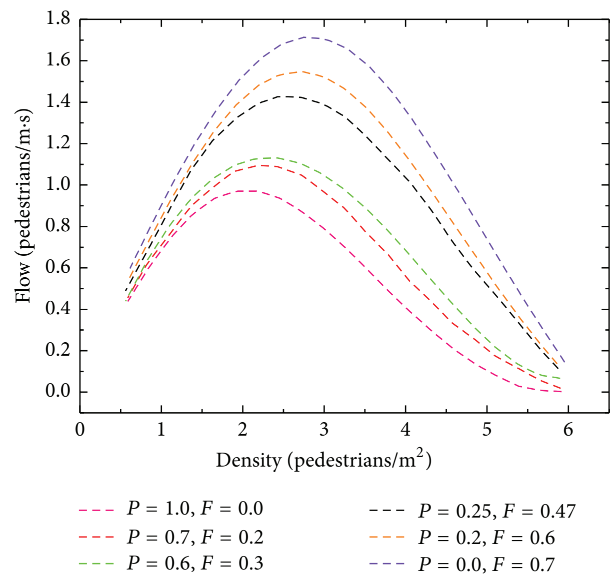

FIGURE 11: Fundamental diagrams of different heterogeneous parameter combination.

of 0.8. We can conclude that F-pedestrians have positive impact on the walkway capacity from Figures 9(b) and 10. The mobility of the walkway improves because of the increasing average speed of pedestrians. These two classes of pedestrians cooperate during the walking process when the proportion of F-pedestrians is low. But when the ratio becomes larger and larger, more and more F-pedestrians want to exceed O-pedestrians and they change their paths frequently which may change the regime of the pedestrian flow. Pedestrians start to compete when they want to go through the same site. This results in the capacity keeping unchanged and even decreasing.

5.4. The Effects of Different Pedestrian Composition on Pedestrian Dynamics. The pedestrian flow would not have only one type of people because of the random composition of pedestrian crowd in reality. The real pedestrian flow is formed of pedestrians with heterogeneous characteristics. To research the effects of different pedestrian composition on pedestrian dynamics, it needs to set the value of parameters P, F, and O to simulate the pedestrian flow under every combination. According to the condition that $P + (1 - P) \times (F + O) = 100\%$, $P \in [0, 1]$, $F \in [0, 1]$, and $O \in [0, 1]$. We set parameters at 0.1 intervals and simulate different parameter combination. The results are shown in Figures 11 and 12.

The result of the experiment shows that the capacity of the walkway ranges from 0.97 to 1.72, and the capacity of pedestrian flow with optimal composition is 77.3% higher than that of pedestrian flow with worst composition.

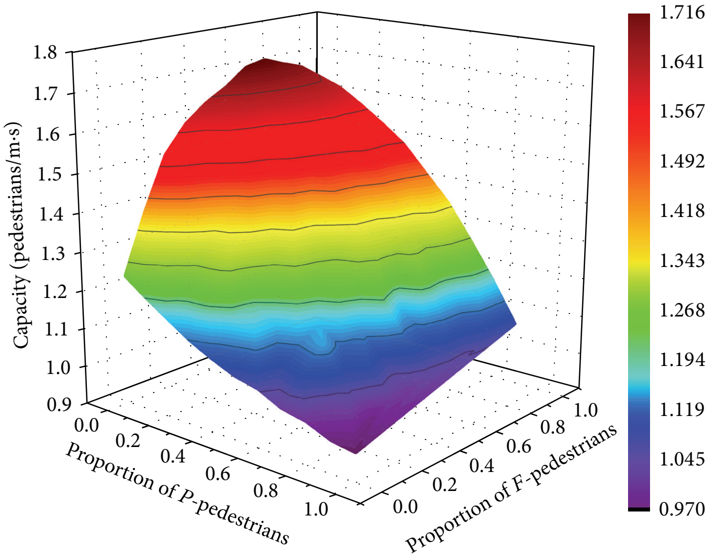

Figure 12: The contour map of capacity under all kinds of heterogeneous parameter combinations.

The highest capacity is occupied when the pedestrian flow consists of F-pedestrians and O-pedestrians with the ratio being 7 to 3. And we get the lowest capacity when there exist only P-pedestrians. In Figure 11, the curves of fundamental diagrams move up and the capacity increases with less P-pedestrians and more F-pedestrians in pedestrian flow. The combination of $P = 0.25$, $F = 0.47$ is the proportion of the observed data. The result indicates again that F-pedestrians have the positive effect on the capacity and P-pedestrians have the opposite effect.

We analyze the contour map of the capacity of pedestrian flow in detail. In Figure 12, when the proportion of P-pedestrians ranges from 0% to 50%, the capacity is between 1.06 and 1.72 and when the percentage ranges from 80% to 100%, the capacity is between 0.97 and 1.17. The results indicate that the features of pedestrian flow are related to the proportion of pedestrians with different heterogeneous characteristics. When the proportion of P-pedestrians in the pedestrian flow is large, F-pedestrians will have less influence. However, if the percentage of P-pedestrians is in a comparatively small range (less than 50%), F-pedestrians will have a big influence. Another conclusion is that about one-third of the results is larger than the capacity stipulated in the *Code for Design of Metro* (the capacity of the unidirectional walkway is 1.39 pedestrians/m·s) of China. It is necessary to take measures to prevent the critical situation caused by some specific composition of heterogeneous pedestrians.

6. Conclusions

In this paper, heterogeneous floor field (HFF) model is proposed to research the pedestrian dynamics of a walkway in Xizhimen subway station. By introducing the pedestrian heterogeneity and analyzing the observed data, we classify the pedestrians into three classes, that is, P-pedestrians, F-pedestrians, and O-pedestrians, according to the heterogeneous characteristics of walking speed and space occupied. We validate the precision of the proposed model under the homogeneous and heterogeneous conditions. In order to explore the effects of different heterogeneous characteristics on the pedestrian dynamics, we compared the critical density, fundamental diagrams, and the capacity of pedestrian flow caused by different composition of pedestrians. The existence of the P-pedestrians has negative effect on the pedestrian flow. With the increasing proportion of P-pedestrians, the trend of the fundamental diagrams and the capacity decline continually. By contrast, the F-pedestrians have the positive influence on the whole. The capacity improves with the increasing proportion of F-pedestrians. But the capacity begins to decrease when the percentage of F-pedestrians is larger than 0.8. It reflects that pedestrians start to compete for the spaces and the pedestrian flow is unstable with high ratio of F-pedestrians. In addition, in order to explore the effects of different combination of heterogeneous parameters that may occur in reality on the pedestrian flow, we made the simulation experiment. The results show that F-pedestrians have a big influence when the percentage of P-pedestrians is less than 50%, and when the proportion of P-pedestrians is larger than 80% F-pedestrians have less influence. Another noteworthy result is that about one-third of the capacity is larger than the value stipulated in the *Code for Design of Metro* of China.

All of the results in this paper indicate that the capacity of walkway is not a constant value. It changes with different component proportions of heterogeneous pedestrians. The heterogeneity of pedestrian has an important influence on the pedestrian dynamics in the walkway of the subway station. These researches can help us understand the macroscopic features of pedestrian flow. They are also beneficial for the operators to take precautions for the emergency caused by special composition of heterogeneous pedestrians in the built stations. And for the unbuilt stations, we can forecast the component proportion of heterogeneous pedestrians in the planning stage to improve the design and construction. In our future work, the presented model will be extended and applied to research the pedestrian dynamics of other facilities in subway stations.

Competing Interests

The authors declare that there is no conflict of interests regarding the publication of this paper.

Acknowledgments

This paper is supported by National Basic Research Program of China (no. 2012CB725403).

References

[1] D. Helbing, P. Molnár, I. J. Farkas, and K. Bolay, "Self-organizing pedestrian movement," *Environment and Planning B: Planning and Design*, vol. 28, no. 3, pp. 361–383, 2001.

[2] A. Schadschneider, A. Kirchner, and K. Nishinari, "CA approach to collective phenomena in pedestrian dynamics," in *Cellular Automata*, vol. 2493 of *Lecture Notes in Computer Science*, pp. 239–248, Springer, New York, NY, USA, 2002.

[3] S. Nowak and A. Schadschneider, "Quantitative analysis of pedestrian counterflow in a cellular automaton model," *Physical Review E*, vol. 85, no. 6, Article ID 066128, 2012.

[4] M. Muramatsu, T. Irie, and T. Nagatani, "Jamming transition in pedestrian counter flow," *Physica A: Statistical Mechanics and Its Applications*, vol. 267, no. 3, pp. 487–498, 1999.

[5] Y. Tajima, K. Takimoto, and T. Nagatani, "Pattern formation and jamming transition in pedestrian counter flow," *Physica A: Statistical Mechanics and Its Applications*, vol. 313, no. 3-4, pp. 709–723, 2002.

[6] K. Takimoto, Y. Tajima, and T. Nagatani, "Effect of partition line on jamming transition in pedestrian counter flow," *Physica A: Statistical Mechanics and Its Applications*, vol. 308, no. 1–4, pp. 460–470, 2002.

[7] H. Kuang, T. Song, X.-L. Li, and S.-Q. Dai, "Subconscious effect on pedestrian counter flow," *Chinese Physics Letters*, vol. 25, no. 4, p. 1498, 2008.

[8] T. Nagatani, "Freezing transition in bi-directional CA model for facing pedestrian traffic," *Physics Letters, Section A: General, Atomic and Solid State Physics*, vol. 373, no. 33, pp. 2917–2921, 2009.

[9] Y. Tajima, K. Takimoto, and T. Nagatani, "Scaling of pedestrian channel flow with a bottleneck," *Physica A: Statistical Mechanics and its Applications*, vol. 294, no. 1-2, pp. 257–268, 2001.

[10] D. Helbing and P. Molnár, "Social force model for pedestrian dynamics," *Physical Review E*, vol. 51, no. 5, pp. 4282–4286, 1995.

[11] D. Helbing, L. Buzna, A. Johansson, and T. Werner, "Self-organized pedestrian crowd dynamics: experiments, simulations, and design solutions," *Transportation Science*, vol. 39, no. 1, pp. 1–24, 2005.

[12] D. Helbing, A. Johansson, and H. Z. Al-Abideen, "Dynamics of crowd disasters: An Empirical Study," *Physical Review E—Statistical, Nonlinear, and Soft Matter Physics*, vol. 75, no. 4, Article ID 046109, 2007.

[13] V. J. Blue and J. L. Adler, "Emergent fundamental pedestrian flows from cellular automata microsimulation," *Transportation Research Record*, no. 1644, pp. 29–36, 1998.

[14] V. J. Blue and J. L. Adler, "Cellular automata microsimulation of bidirectional pedestrian flows," *Transportation Research Record*, no. 1678, pp. 135–141, 1999.

[15] V. J. Blue and J. L. Adler, "Cellular automata microsimulation for modeling bi-directional pedestrian walkways," *Transportation Research Part B: Methodological*, vol. 35, no. 3, pp. 293–312, 2001.

[16] M. Fukui and Y. Ishibashi, "Jamming transition in cellular automaton models for pedestrians on passageway," *Journal of the Physical Society of Japan*, vol. 68, no. 11, pp. 3738–3739, 1999.

[17] M. Fukui and Y. Ishibashi, "Self-organized phase transitions in cellular automaton models for pedestrians," *Journal of the Physical Society of Japan*, vol. 68, no. 8, pp. 2861–2863, 1999.

[18] B. Chopard and M. Droz, *Cellular Automata Modeling of Physical Systems*, vol. 6, Cambridge University Press, Cambridge, Mass, USA, 2005.

[19] D. H. Rothman and S. Zaleski, "Lattice-gas models of phase separation: interfaces, phase transitions, and multiphase flow," *Reviews of Modern Physics*, vol. 66, no. 4, pp. 1417–1479, 1994.

[20] H.-H. Tian, H.-D. He, Y.-F. Wei, X. Yu, and W.-Z. Lu, "Lattice hydrodynamic model with bidirectional pedestrian flow," *Physica A: Statistical Mechanics and Its Applications*, vol. 388, no. 14, pp. 2895–2902, 2009.

[21] S. Bandini, S. Manzoni, and G. Vizzari, "Agent based modeling and simulation," in *Encyclopedia of Complexity and Systems Science*, pp. 184–197, Springer, New York, NY, USA, 2009.

[22] M. Batty, B. Jiang, and M. Thurstain-Goodwin, *Local Movement: Agent-based Models of Pedestrian Flows*, 1998.

[23] C. Burstedde, K. Klauck, A. Schadschneider, and J. Zittartz, "Simulation of pedestrian dynamics using a two-dimensional cellular automaton," *Physica A: Statistical Mechanics and Its Applications*, vol. 295, no. 3-4, pp. 507–525, 2001.

[24] A. Kirchner and A. Schadschneider, "Simulation of evacuation processes using a bionics-inspired cellular automaton model for pedestrian dynamics," *Physica A: Statistical Mechanics and Its Applications*, vol. 312, no. 1-2, pp. 260–276, 2002.

[25] A. Kirchner, K. Nishinari, and A. Schadschneider, "Friction effects and clogging in a cellular automaton model for pedestrian dynamics," *Physical Review E*, vol. 67, no. 5, Article ID 056122, 2003.

[26] A. Schadschneider, D. Chowdhury, and K. Nishinari, *Stochastic Transport in Complex Systems: From Molecules to Vehicles*, Elsevier, New York, NY, USA, 2010.

[27] A. Tsiftsis, I. G. Georgoudas, and G. C. Sirakoulis, "Real data evaluation of a crowd supervising system for stadium evacuation and its hardware implementation," *IEEE Systems Journal*, vol. 10, no. 2, pp. 649–660, 2015.

[28] I. G. Georgoudas, G. C. Sirakoulis, and I. T. Andreadis, "An anticipative crowd management system preventing clogging in exits during pedestrian evacuation processes," *IEEE Systems Journal*, vol. 5, no. 1, pp. 129–141, 2011.

[29] H. Klüpfel and T. Meyer-König, "Simulation of the evacuation of a football stadium using the CA model PedGo," in *Proceedings of the 5th International Workshop on Traffic and Granular Flow (TGF '03)*, pp. 423–428, October 2003.

[30] J. Wąs, R. Lubaś, and W. Myśliwiec, "Proxemics in discrete simulation of evacuation," in *Cellular Automata*, pp. 768–775, Springer, Berlin, Germany, 2012.

[31] Y.-C. Qu, Z.-Y. Gao, Y. Xiao, and X.-G. Li, "Modeling the pedestrian's movement and simulating evacuation dynamics on stairs," *Safety Science*, vol. 70, pp. 189–201, 2014.

[32] M. Campanella, S. Hoogendoorn, and W. Daamen, "Quantitative and qualitative validation procedure for general use of pedestrian models," in *Pedestrian and Evacuation Dynamics 2012*, pp. 891–905, Springer, 2014.

[33] L.-L. Lu, G. Ren, W. Wang, and Y. Wang, "Modeling walking behavior of pedestrian groups with floor field cellular automaton approach," *Chinese Physics B*, vol. 23, no. 8, Article ID 088901, 2014.

[34] M. Campanella, S. P. Hoogendoorn, and W. Daamen, "Effects of heterogeneity on self-organized pedestrian flows," *Transportation Research Record*, no. 2124, pp. 148–156, 2009.

[35] M. Matsumoto, M. Miska, M. Kuwahara, and S. Tanaka, "Microscopic pedestrian simulation considering heterogeneity," in *Proceedings of the 12th World Conference on Transport Research (WCTR '10)*, Lisbon, Portugal, July 2010.

[36] A. Schadschneider, H. Klüpfel, T. Kretz, C. Rogsch, and A. Seyfried, "Fundamentals of pedestrian and evacuation dynamics," in *Multi-Agent Systems for Traffic and Transportation Engineering*, pp. 124–154, 2009.

[37] A. Seyfried, B. Steffen, W. Klingsch, and M. Boltes, "The fundamental diagram of pedestrian movement revisited," *Journal of Statistical Mechanics: Theory and Experiment*, no. 10, Article ID P10002, pp. 41–53, 2005.

[38] A. Schadschneider, A. Kirchner, and K. Nishinari, "From ant trails to pedestrian dynamics," *Applied Bionics and Biomechanics*, vol. 1, no. 1, pp. 11–19, 2003.

[39] Y. Zheng, B. Jia, X.-G. Li, and N. Zhu, "Evacuation dynamics with fire spreading based on cellular automaton," *Physica A: Statistical Mechanics and Its Applications*, vol. 390, no. 18-19, pp. 3147–3156, 2011.

[40] D.-F. Xie, Z.-Y. Gao, X.-M. Zhao, and D.-Z. Wang, "Cellular automaton modeling of the interaction between vehicles and pedestrians at signalized crosswalk," *Journal of Transportation Engineering*, vol. 138, no. 12, pp. 1442–1452, 2012.

[41] I. G. Georgoudas, G. Koltsidas, G. C. Sirakoulis, and I. T. Andreadis, "A cellular automaton model for crowd evacuation and its auto-defined obstacle avoidance attribute," in *Cellular Automata*, pp. 455–464, Springer, Berlin, Germany, 2010.